A&A 516, A73 (2010)
DOI: 10.1051/0004-6361/200913703

Astronomy & Astrophysics

Evolution of two stellar populations in globular clusters

II. Effects of primordial gas expulsion

T. Decressin[1], H. Baumgardt[1,⋆], C. Charbonnel[2,3], and P. Kroupa[1]

[1] Argelander Institute for Astronomy (AIfA), Auf dem Hügel 71, 53121 Bonn, Germany
e-mail: decressin@astro.uni-bonn.de
[2] Geneva Observatory, University of Geneva, 51 ch. des Maillettes, 1290 Versoix, Switzerland
[3] Laboratoire d'Astrophysique de Toulouse-Tarbes, CNRS UMR 5572, Université de Toulouse, 14 Av. E. Belin, 31400 Toulouse, France

Received 19 November 2009 / Accepted 23 March 2010

ABSTRACT

Aims. We investigate the early evolution of two distinct populations of low-mass stars in globular clusters under the influence of primordial gas expulsion driven by supernovae and study whether this process can increase the fraction of second generation stars at the level required by observations.
Methods. We analyse N-body models that take the effect of primordial gas expulsion into account. We divide the stars into two populations that mimic the chemical and dynamical properties of stars in globular clusters so that second-generation stars start with a more centrally concentrated distribution.
Results. The main effect of gas expulsion is to eject mostly first-generation stars while second-generation stars remain bound to the cluster. In the most favourable cases, second-generation stars can account for 60% of the bound stars we see today. We also find that, at the end of the gas expulsion phase, the radial distribution of the two populations is still different, so that long-term evolution will further increase the fraction of second generation stars.
Conclusions. The large fraction of chemically anomalous stars is readily explainable as a second generation of stars formed out of the slow winds of rapidly rotating massive stars if globular clusters suffer explosive residual gas expulsion for a star formation efficiency of about 0.33.

Key words. globular clusters: general – stellar dynamics – methods: numerical

1. Introduction

Globular clusters (GCs) are self-gravitating aggregates of tens of thousands to millions of stars that have survived over a Hubble time. Many observations show that these objects are composed of (at least) two distinct stellar populations. The first evidence rests on the chemical analysis that reveals large star-to-star abundance variations in light elements in all individual clusters studied so far, while the iron abundance stays constant (for a review see Gratton et al. 2004). This includes the well-documented anticorrelations between C-N, O-Na, Mg-Al, Li-Na, and F-Na (Kraft 1994; Carretta et al. 2006, 2007, 2009; Gratton et al. 2007; Pasquini et al. 2007; Bonifacio et al. 2007; Lind et al. 2009). This global chemical pattern requires H-burning at high temperatures around 75×10^6 K (Arnould et al. 1999; Prantzos et al. 2007). As the observed chemical pattern is present in low-mass stars, both on the red giant branch (RGB) and at the turn-off, which cannot have reached such high temperatures, the abundance anomalies must have been inherited at the time of formation of these stars.

Further indications of multiple populations in individuals GCs comes from deep photometric studies that have revealed multiple giant branches or main sequences. In ω Cen a blue main sequence has been discovered (Bedin et al. 2004) that is presumably related to a high content in He (Piotto et al. 2005; Villanova et al. 2007). A triple main sequence has been discovered in NGC 2808 (Piotto et al. 2007). A broadening of the main sequence of NGC 6752 has also been discovered, which cannot be explained by binary stars (Milone et al. 2010). The additional blue sequences are only explicable by a higher He content of the corresponding stars, which increases the opacity and shifts the effective temperature towards higher temperatures. He-rich stars are also the progenitors of blue horizontal branch stars seen in many GCs (see Caloi & D'Antona 2005, 2007). Whereas no direct observational link between abundance anomalies and He-rich sequences has been found, theoretically this link is easily understood because abundance anomalies are the main result of H burning to He.

These observed properties lead to the conclusion that GCs created out of giant gas clouds first form a generation of stars with the same abundance pattern as field stars. Then a polluting source enriches the intracluster-medium with H-burning products out of which a chemically-different second stellar generation forms with a spread of chemical peculiarities. This scheme can explain at the same time the abundance anomalies in light elements and He-enrichment.

Two main candidates that reach the right temperature for H-burning have been proposed as the origin of the abundance anomalies (Prantzos & Charbonnel 2006): (a) intermediate-mass stars evolving through the thermal pulses along the asymptotic giant branch (hereafter TP-AGB), and (b) main sequence massive stars. After first being proposed by Cottrell & Da Costa (1981), the AGB scenario has been extensively studied

⋆ *Present address*: Department of Physics, University of Queensland, Brisbane, QLD 4072, Australia.

(Ventura et al. 2001, 2002; Ventura & D'Antona 2005a,b,c, 2008a,b, 2009; Denissenkov & Herwig 2003; Karakas & Lattanzio 2003; Herwig 2004a,b; Fenner et al. 2004; Bekki et al. 2007; Decressin et al. 2009). In massive TP-AGB stars ($M \geq 4\ M_{\odot}$), the abundance anomalies are supposed to have been created at the bottom of the convective envelope through hot bottom burning.

On the other hand, as suggested by Wallerstein et al. (1987) and Brown & Wallerstein (1993), massive stars can also pollute the inter-stellar medium (ISM) of a forming cluster (see Smith 2006; Prantzos & Charbonnel 2006). In particular, Decressin et al. (2007b) show that fast-rotating massive stars (with a mass higher than ~25 $M_{\odot}$) are good candidates for the self-enrichment of GCs. In the wind of fast-rotating massive stars (WFRMS) scenario, rotationally-induced mixing transports H-burning products (hence matter with correct abundance signatures) from the convective core to the stellar surface, and, provided initial rotation is high enough, the stars reach break-up velocity while on the main sequence. As a result, a mechanical wind is launched from the equator that generates a disk around the star similar to that of Be stars (e.g. Townsend et al. 2004). Later, when He-burning products are brought to the surface, the star has already lost a high fraction of its initial mass and angular momentum, so that it no longer rotates at the break-up velocity. Matter is then ejected through a classical fast isotropic radiative wind. From the matter lost through the disk, a second generation of stars may be created with a chemical pattern that agrees with observations.

In the present paper we mainly focus on the dynamical constraints related to the WFRMS scenario. However, both scenarios face a similar problem. Within standard assumptions (canonical IMF and conservation of the stars in the cluster), the amount of matter lost by the polluter stars is much less than the mass locked into the first-generation low-mass stars. Indeed, if we assume that first-generation massive stars follow the canonical IMF[1], stars in the mass range 25–120 $M_{\odot}$ account for only 10% of the mass of the whole first stellar generation (see Decressin et al. 2007a) and their slow winds account for only 2.5% of the mass. If pollution is due to AGB stars, a similar constraint arises: the wind released by stars between 5 and 6.5 $M_{\odot}$ represents less than 3%, for which nucleosynthesis agrees with the observations according to Ventura & D'Antona (2008a). After taking the possible dilution of these slow winds into account with the pristine gas present in the ISM to explain the observed Li abundance variation (Decressin et al. 2007a), we find that the mass available to form the second-generation low-mass stars compared to the first-generation of low-mass stars is only about 10%. This is in sharp contrast with observations, which show that more than half and up to 85% of the stars in GCs are second-generation stars (Prantzos & Charbonnel 2006; Carretta et al. 2009), i.e., which show anticorrelations in light elements. Thus a rather extreme reduction in the first-generation stars relative to the second generation stars is needed to reproduce the observations. However, massive binaries have recently been proposed as polluters of the proto-GC by de Mink et al. (2009). In this case the mass-budget is more favourable as more slow winds are ejected and more second generation stars are formed. This could help to reduce the fraction between first and second-generation stars found in the present paper, thereby supporting a high-mass star pollution scenario.

One possible way to reconcile the pollution scenario with the observations is to consider a top-heavy initial mass function (IMF) of first-generation stars. In the case of pollution by fast-rotating massive stars, an IMF slope as flat as 1.55 (compared to the canonical value of 2.3) is required to reproduce the high number of stars with abundance anomalies in the cluster NGC 6752 (Decressin et al. 2007a), whereas the AGB scenario requires an even flatter IMF slope (see Prantzos & Charbonnel 2006).

A second way to reconcile the pollution scenario with observations is to consider that first-generation stars are primarily lost from the cluster during its evolution so that an initially relatively small population of second-generation stars can become the dominant population after several Gyr. To allow this preferential loss of first generation stars requires the GCs to initially be mass-segregated (i.e., that more massive stars occupy the central part of the clusters). In this case the matter released in the disks of massive stars is more concentrated in the cluster centre, and second-generation stars are born in the centre, while first-generation stars are present throughout the cluster.

The viability of a self-enrichment scenario by fast-rotating massive stars has recently been explored by Decressin et al. (2008, Paper I). They have shown that first-generation low-mass stars are mainly lost from the cluster, which is assumed to initially be in dynamical equilibrium and mass-segregated, before two-body relaxation induces a spread of second generation stars and a full mixing of the cluster. D'Ercole et al. (2008) find similar results with the AGB scenario. Afterwards, the evolution is smoother and the variation in the fraction of second-generation stars takes longer. Any radial difference between first and second generation stars is erased after 10–12 Gyr of evolution because the cluster relaxation time (a few Gyr) is much shorter than the age of the clusters[2]. In Paper I we show that, even if the relaxation-driven evaporation increases the fraction of second generation (which harbour abundance anomalies) to about 25%, this ratio remains too low to fully explain the observations (between 50–85%, Carretta et al. 2009). The increase in the fraction of second-generation stars mainly occurs in the early times and points towards the high sensitivity of the fraction of second-generation stars on cluster dynamics.

In this paper, we aim to quantify the increase in the fraction of second-generation stars to the total number of low-mass stars by another dynamical mechanism not taken into account in the above studies, namely the effect of primordial gas expulsion (i.e., the fast ejection of the remaining gas left by star formation after the onset of supernovae, see e.g., Tutukov 1978). Gas expulsion can strongly modify the total binding energy of the cluster and can lead to an efficient loss of first-generation stars from the cluster. We emphasise that we discuss generic properties of gas expulsion models based on the simplified assumption that a cluster contains only two stellar generations with the same [Fe/H]. Multiple populations with different [Fe/H] would require other physical mechanisms, whereby notably gas accretion form the surrounding interstellar medium (Pflamm-Altenburg & Kroupa 2009) may play a role, as well as recycling of SN ejecta (Tenorio-Tagle et al. 2007). In Sect. 2 we present the N-body models used in this study. Then our results are discussed in

[1] The canonical IMF is a two-part power-law function, $f(m) \propto m^{-\alpha_i}$, with $\alpha_1 = 1.3$ for stellar masses $0.08 \leq m/M_{\odot} \leq 0.5$ and $\alpha_2 = 2.3$ (Salpeter value) for $m > 0.5\ M_{\odot}$ (Kroupa 2001).

[2] The only exception is the GC ω Cen, for which the relaxation time at the center is comparable to its age. Indeed in this cluster stars on the blue main sequence (i.e., He-rich) are found more centrally concentrated than red main sequence stars (Villanova et al. 2007; Bellini et al. 2009).

Sect. 3. In Sect. 4 we present a complete scenario for the evolution of GCs and our conclusions are founded in Sect. 5.

2. Description of analysis

The results presented in this paper are based on the grid of N-body models computed by Baumgardt & Kroupa (2007), where the effects of primordial gas expulsion on the dynamics of star clusters were studied. The N-body models are computed with the NBODY4 code (Aarseth 1999) and follow the evolution of 20 000 single-mass stars. The gas is treated as a spherical additional potential that is removed gradually in order to change the total binding energy of the cluster. The initial cluster follows a Plummer distribution. The cluster evolution is computed for 100 to 150 initial crossing times so that the cluster can settle into a new equilibrium configuration and two-body relaxation (which acts on a much longer timescale) is not an important parameter in these models.

Baumgardt & Kroupa (2007) studied in particular the influence of three physical parameters on the early cluster dynamics. The first is the star formation efficiency, ϵ, given by the ratio between the stellar mass and the initial mass of the parent gas cloud. This parameter defines the fraction of gas converted into stars by star formation. The second parameter is the ratio between the half-mass radius and the tidal radius, $r_{\rm h}/r_{\rm t}$, which quantifies the initial concentration of the cluster and the strength of the tidal field of the host Galaxy. Finally, the third parameter is the ratio of the timescale for gas expulsion relative to the crossing time, $\tau_{\rm GE}/t_{\rm cr}$. This quantity determines the ability of stars to adjust their orbital parameters when the potential changes during gas expulsion. The full grid of models includes variation in the star formation efficiency between 0.05 and 0.75, of the ratio of the half-mass radius to the tidal radius between 0.01 and 0.2, and of the ratio of the timescale for gas expulsion relative to the crossing time between 0 and 10.

As the models of Baumgardt & Kroupa (2007) take only one stellar population into account, we use the same method as in Paper I to split the stars into two populations according to their specific energy. The stars with the highest binding energy mimic second-generation stars that are more centrally concentrated, while the other stars are assumed to be members of the first generation. We choose an initial fraction of second generation stars of 10% to be consistent with the pollution by fast-rotating massive stars in the case of a canonical IMF slope. As Baumgardt & Kroupa (2007) used only single-mass stars, we cannot study in detail the mass dependence of our results. However, the gas expulsion process we investigate here (duration shorter than 10 crossing times) acts on a much shorter timescale than two-body relaxation (a few Gyr), which could lead to the preferential loss of low-mass stars, and also acts on a shorter timescale than the lifetime of low-mass stars, so we do not expect our results to depend much on the mass of the stars. Similarly, the short duration of the gas expulsion phase compared to the two-body relaxation timescale allows us to infer results suitable for the study of the early dynamics of GCs even with the limited number of stars (20 000) in the N-body model library.

3. Results

3.1. Analysis of individual models

Baumgardt & Kroupa (2007) find that gas expulsion can lead to all situations between a cluster totally disrupted and an unaffected cluster, depending on the parameter values for the gas-expulsion timescale $\tau_{\rm GE}$, the star formation efficiency ϵ, and cluster concentration c. In this paper we concentrate on intermediate cases that predict a large stellar mass loss but with a remnant dense core. In Fig. 1 we present three such interesting cases.

Case 1. The left panels show predictions for the gas expulsion parameters $\epsilon = 0.2$, $c = r_{\rm h}/r_{\rm t} = 0.01$, and $\tau_{\rm GE}/t_{\rm cr} = 1$, which represent an initially concentrated cluster with a low star formation efficiency and a long timescale for gas expulsion. In the upper left panel we show the evolution of the number of stars of the first and second population still bound to the cluster. We use the following criteria to define whether, at a given time, a star is bound to the cluster: the star needs to be within the tidal radius of the cluster and to have a negative total energy (sum of the kinetic and potential energy). Initially, some stars have a positive total energy and move away from the cluster. However, during about the first 10 crossing times the radius of the stars bound to the cluster expands so that these stars stay within the cluster tidal radius. During the first 30 crossing times, about 10% of the stars are in this situation (positive total energy and still within the tidal radius of the cluster), and it depends on the criteria used if they are to be considered as bound (Baumgardt & Kroupa 2007, with only a radius criterium) or unbound (this study with both a radius and an energy criterium). However, after around 30 crossing times, both criteria give the same results so that at the end of the computation no difference exists between both criteria. The two-phase decrease in the number of stars comes from the change of an energy-dominating criterion in the early times to a radial criterion that dominates after 30 crossing times. Using only the radial criterion would have led to a smoother decrease in the number of bound stars (see Baumgardt & Kroupa 2007).

As expected from the initial radial distribution, case 1 depicts a cluster that loses more of its first-generation stars (about 80%) than second-generation ones (about 12%) so that the fraction of second-generation stars is around 30% at the end of the computation (middle left panel in Fig. 1). The loss of stars is very pronounced during the first few crossing times when the lowering of the cluster binding energy is driven by the gas expulsion.

An interesting point is that the radial distributions (see left bottom panel in Fig. 1) differ at the end of the simulation (about 100 initial crossing times), since second-generation stars are still more concentrated than the first-generation ones. Thus we can expect that the fraction of second-generation stars will increase further owing to the relaxation-driven long-term evaporation of the clusters, as seen in Paper I. Moreover, the final radius of the cluster is much larger than initially. Indeed the half-mass radius of first and second generation stars is 1.0 and 0.6 pc, respectively at $t = 0$, and becomes 8.5 and 3.8 pc at the end of the computation. This strong radial expansion by a factor 8.4 (first generation) and 6.3 (second generation) is mainly caused by the long timescale for gas expulsion, $\tau_{\rm GE}$, that is similar to the crossing time, allowing stars to adopt new orbital parameters with wider orbits without being lost from the cluster. It should be noted that the tidal field is also weak in this case as shown by the radial extension of the cluster up to about 30 times its initial half-mass radius.

Case 2. The central panels of Fig. 1 present the case of a cluster near total disruption, which loses ~95% of its first-generation stars owing to the gas expulsion process. The initial parameters are $\epsilon = 0.30$, $r_{\rm h}/r_{\rm t} = 0.033$, and $\tau_{\rm GE}/t_{\rm cr} = 0.33$. Compared to the previous case, this model has a smaller gas fraction after star formation, and gas expulsion occurs on a much shorter timescale. As this cluster shows a smaller increase in its radius

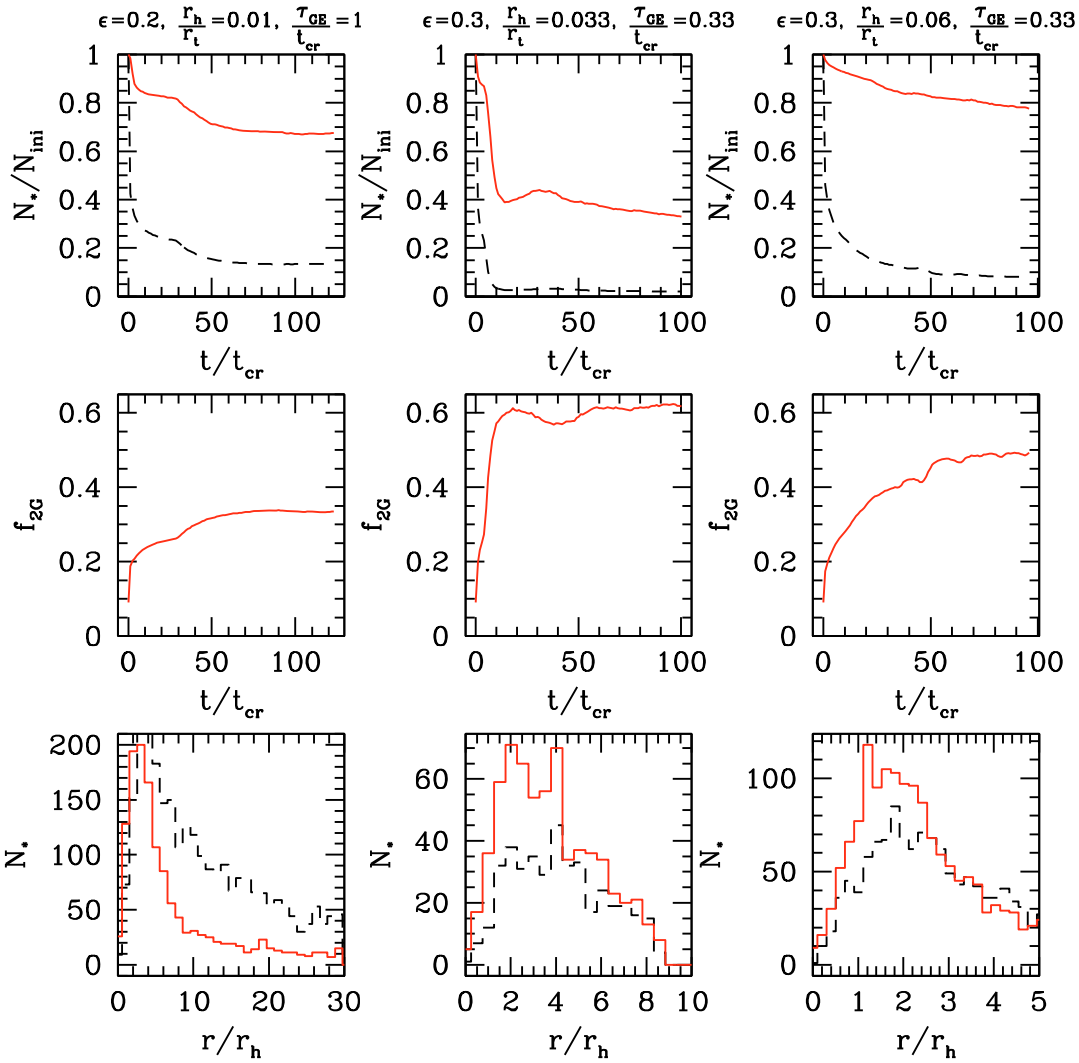

Fig. 1. *Top panels*: number fraction of first (dashed lines) and second generation (full lines) stars relative to their initial number as a function of time. Each line is normalised to its initial number. *Middle panel*: fraction of second generation stars bound to the cluster as a function of time. *Bottom panel*: final (at 100 initial crossing times) radial distribution from the cluster centre for the stars of the first (dashed lines) and the second (full lines) generation. Right, central, and left panels refer to three cases with different initial parameters indicated at the top.

during its evolution, the two-phase decrease in the number of stars is limited to only the first 5 crossing times. The number of bound stars goes through a minimum around 10 crossing times before increasing during the following 20 crossing-times. This behaviour is related to the strong ellipsoidal shape that the cluster displays during its expansion phase, leading to a significant number of stars lying in the outer part of the major axis of the cluster distribution where they are outside the tidal radius (so are counted as unbound stars). When the cluster contracts and becomes more spherical, part of these stars decrease their orbital radius below r_t and become bound to the cluster again. At the end of the evolution, the cluster radius has only increased by a factor 3–4. The central part of the cluster is dominated by second-generation stars (bottom panel) and the fraction of second generation stars at the end is above 60%. However, because of the low number of bound stars in the simulation, statistics becomes too poor to precisely infer cluster properties.

Case 3. Finally the right panels of Fig. 1 correspond to a model with initial parameters of $\epsilon = 0.33$, $r_h/r_t = 0.06$, and $\tau_{GE}/t_{cr} = 0.33$ that also undergoes a strong loss of stars leading to a cluster with second-generation stars counting for half of all cluster members. This case is particularly interesting as it has a small final half-mass radius that is only about twice the initial half-mass radius. Second-generation stars dominate at the centre, so we can expect that the further evolution of this cluster will increase the fraction of second-generation stars to match the observed fraction (50–85%) of stars with anticorrelations in light elements when taking its whole evolution into account.

3.2. The whole set of models

Figure 2 (left panel) shows the fraction of second-generation stars remaining bound after gas expulsion, $f_{2G} = N_2/(N_1 + N_2)$, as a function of the fraction of remaining bound stars, $f_{bound} = (N_1+N_2)/N_{ini}$. All cases are located between two extreme scenarios: no loss of second-generation stars (upper dashed line) and no preferential loss of first-generation stars (horizontal dashed line). All the cases computed by Baumgardt & Kroupa (2007) that have more than 100 bound stars at the end of the integration are presented. To assess the statistical significance of the results, we estimate the statistical error from $\sigma = \sqrt{\sigma_1^2 + \sigma_2^2}$, where $\sigma_1 = N_1^{-0.5}$ and $\sigma_2 = N_2^{-0.5}$ are the statistical uncertainties for the number of first and second generation stars. In clusters

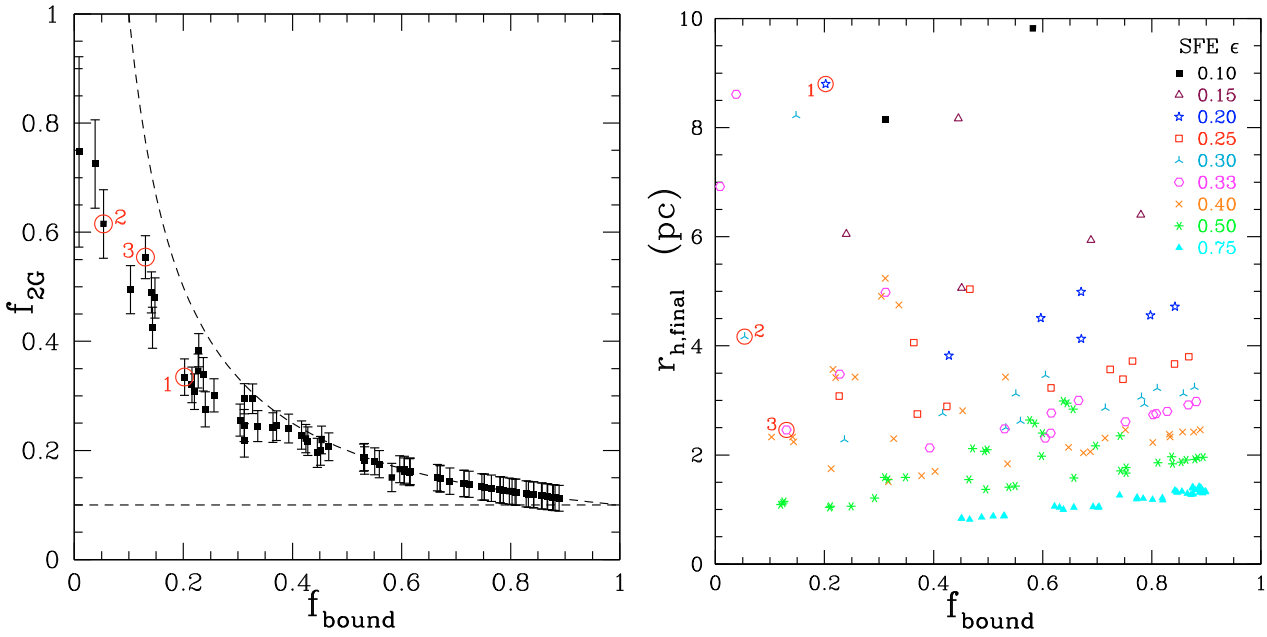

Fig. 2. *Left*: fraction of second-generation stars as a function of the final fraction of bound stars at the end of the computations of Baumgardt & Kroupa (2007), i.e., after about 100 initial crossing times. Dashed lines indicate limiting cases where no second-generation stars are lost (*upper*) and no preferential loss of first-generation stars occurs (*lower*). Estimates of the statistical errors are also included based on the number of first, N_1, and second, N_2, generation stars bound to the cluster. *Right*: final half-mass radius of the cluster as a function of the fraction of bound stars at the end of the computation. Clusters with different values of the star formation efficiency, ϵ, are indicated with various symbols and colours. In both figures, numbered circles indicate the three models presented in Fig. 1 and discussed in Sect. 3.1.

that do not lose many stars (points on the right), the error is dominated by σ_2, while σ_1 and σ_2 contribute significantly for clusters suffering a large loss of stars. For clusters with fewer than 500 stars, the remaining error is about 20%.

A general trend is clearly visible in that the more dissolved clusters also have a higher fraction of second-generation stars at the end. This behaviour is expected since second-generation stars are initially more bound to the cluster and the gas expulsion occurs on a shorter timescale than the two-body relaxation timescale. For clusters near disruption, the fraction of second-generation stars can be as high as 70–75%, although with poor statistics. *N*-body simulations with more initial stars will be very helpful for quantifying these numbers more precisely.

Even if the fraction of second-generation stars is a monotonic function of the fraction of stars remaining bound to the cluster, other cluster properties present a more pronounced dependence with the initial parameters. Figure 2 (right panel) shows the final half-mass radius of the cluster as a function of the fraction of stars remaining bound to the cluster. For clusters with high $f_{\rm bound}$, the half-mass radius increases with decreasing value of the star formation efficiency. Indeed clusters with a high star formation efficiency are less perturbed when the primordial gas expulsion happens because of a lower mass of the gas remaining after star formation. This trend roughly remains at low ϵ value but with more scatter.

3.3. Initial conditions for globular cluster formation

Figure 3 shows the fraction of second-generation stars that remain bound to the cluster after the end of the gas expulsion phase for all the input parameters used by Baumgardt & Kroupa (2007). White areas indicate fully disrupted clusters, while yellow to red colours indicate the fraction of second-generation stars at the end of the computation. By varying the SFE, we retrieve the three main behaviours for clusters. For clusters with low SFE (ϵ between 0.05 and 0.1), almost no cluster can survive. In contrast, gas expulsion has almost no effect on high SFE cases (see bottom right panel with SFE of $\epsilon = 0.75$). In this last case, f_{2G} always remains lower than 20%.

Intermediate values of the SFE around 0.3–0.33 are more interesting, since many cases lead to a high fraction of second-generation stars still bound to the cluster. For an SFE of 0.33, a high fraction of second-generation stars relative to cluster stars is obtained for concentrated clusters with a short timescale for gas expulsion ($\tau_{\rm GE}/t_{\rm cr} \leq 1$). These candidates could be good progenitors of real GCs (see second and third cases in Fig. 1 in Sect. 3.2). It should be noted that a value of 0.33 for the SFE is close to the one found by Parmentier & Fritze (2009) from their study of the mass evolution of clusters and is also consistent with direct observational surveys (Lada & Lada 2003). As we have seen, clusters with a low $r_{\rm h}/r_{\rm t}$ ratio are more prone to present an high fraction of second generation stars. Thus this fraction should be higher with large distance to the Galactic centre (larger $r_{\rm t}$). Alternatively, the tidal field may have been weaker because the Galaxy had not yet been assembled. The observational trend observed by Carretta (2006), who shows that clusters with large orbital period and with high orbital inclinations relative to the Galactic plane produce more extended O-Na and Mg-Al anticorrelations (see also Fraix-Burnet et al. 2009), could be the imprint of the primordial gas expulsion process.

In addition to an SFE around 0.33, other regions of parameter space favour a large increase in the fraction of second-generation stars, namely an SFE around 0.25 combined with a fast timescale for gas expulsion and a very concentrated cluster ($r_{\rm h}/r_{\rm t} \leq 0.05$). A last possibility is for a higher SFE ($\epsilon = 0.5$) and an initially extended cluster ($r_{\rm h}/r_{\rm t} \geq 0.1$). However, this case produces clusters that are too extended compared to the observed ones, so that only SFEs around or below 0.33 are allowed to increase the fraction of second-generation stars.

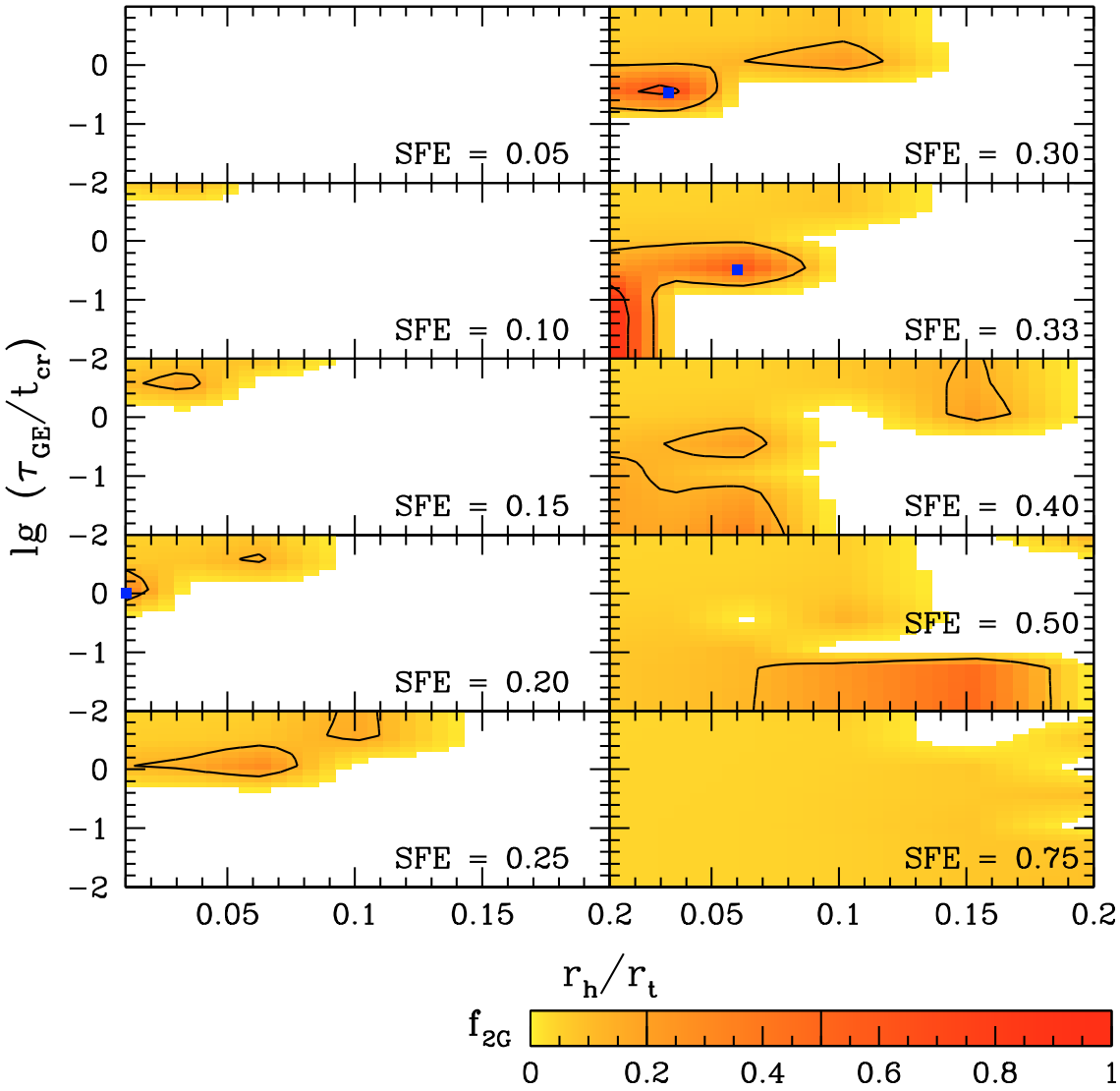

Fig. 3. Fraction of second-generation stars, f_{2G}, which remain bound after gas expulsion as a function of various initial parameters. Each panel has a different value for the star formation efficiency (from 0.05 to 0.75). White areas indicate dissolved clusters (i.e., with less than 100 bound stars). Black lines indicate levels where f_{2G} is equal to 20% (outer contour) and 50% (inner contour). Blue dots in panels SFE = 0.20, 0.30, and 0.33 indicate the three models presented in Fig. 1 (the ratio of the gas expulsion timescale to the crossing time is expressed in decimal logarithm).

4. Towards a complete scenario for the evolution of globular clusters

As we have seen in the previous section, primordial gas expulsion can be a very efficient mechanism to increase the ratio between second and first generation stars. The most favourable physical conditions for GC formation and early evolution are: (1) a star formation efficiency around $\epsilon = 0.33$, (2) a concentrated cluster relative to the tidal radius and (3) a fast timescale for gas expulsion. In the following we would like to consider how these constraints can be used to refine the scenario of the evolution of GCs with pollution by fast-rotating massive stars.

4.1. The wind of fast-rotating massive stars scenario

As already outlined in the introduction, our scenario requires some basic assumptions that are detailed in Decressin et al. (2007a). Let us recall the main points here. We suppose that the first stellar generation contains stars with initial masses between 0.1 and 120 $M_\odot$ following a standard IMF with a Salpeter-like slope for stars more massive than 0.8 $M_\odot$ and a log-normal distribution for lower mass stars (Paresce & De Marchi 2000), but that second-generation stars only consist of low-mass, long-lived stars with initial masses between 0.1 and 0.8 $M_\odot$[3]. We consider that the first-generation polluters are fast-rotating massive stars (i.e., with initial masses above ~25 $M_\odot$) that enrich the ISM through their slow mechanical winds loaded with H-burning products. We assume mass segregation, primordial gas expulsion, and long-term evaporation of first-generation low-mass stars in order to reproduce the large fraction of second-generation long-lived stars we see today (see Sect. 3).

The evolution of GCs passes through different key phases:

1. *Formation of a first-generation of stars*. First-generation stars (over the complete mass range 0.1 to 120 $M_\odot$) form from a giant molecular cloud with a "normal" chemical composition similar to that of contemporary halo field stars of similar metallicity. As shown in Sect. 3, specific conditions

[3] The assumption about the mass range of second-generation stars is made only in order to minimise the constraints on the mass budget.

are required at that phase: (1) an initial star formation efficiency for first-generation stars defined as the total mass enclosed within first-generation stars relative to the initial mass of the proto-cluster cloud in the same volume, ϵ_{1G}, around 0.3–0.33 and (2) an initially highly concentrated cluster with a small half-mass radius (up to a few pc, see Sect. 4.2.4).

2. *Evolution of fast-rotating massive stars ($m > 25\ M_\odot$) and cluster pollution*. Part of the pristine gas that has not been consumed to form first-generation stars must sit within the cluster during the lifetime of the less massive polluters, i.e., ~7–10 Myr for a 25 $M_\odot$ star (see Sect. 4.2.4 below). Indeed the Li-free matter ejected by massive stars in their slow winds has to be mixed with pristine Li-rich, intra-cluster gas in order to explain the Li-Na anticorrelation observed in NGC 6752 (Pasquini et al. 2005) and 47 Tuc (Bonifacio et al. 2007) and NGC 6397 (Lind et al. 2009). This anticorrelation can actually be used to constrain the amount of pristine gas involved in this dilution process (see Sect. 4.2.1).
3. *Formation of second generation stars*. Second-generation low-mass stars (0.1–0.8 $M_\odot$) form from the ISM material polluted to various degrees by the slow winds of massive stars loaded with H-burning products. They have to be more centrally concentrated than their first-generation counterparts, as required by the number ratios between first and second generation objects we observe today. Decressin et al. (2007a) propose that massive polluters of the first generation could be born in the centre of the cluster or could have migrated there rapidly through mass segregation. In both cases, the second-generation stars are created in their immediate vicinity and share a similar radial distribution. Here we define the formation efficiency of the second stellar generation, ϵ_{2G}, as the ratio of the total mass enclosed by second-generation stars to the total mass of the slow winds ejected by massive stars and the ISM matter used for the dilution process.
4. *Gas expulsion by SN*. Then gas expulsion occurs and removes the interstellar gas left after the two episodes of star formation[4]. For this process to be efficient enough, the gas expulsion timescale must be very short, i.e., in the explosive regime, $\tau_{GE} < t_{cr}$ (see Sect. 3). We propose that this process is induced by the supernova explosions of the first-generation stars that did not contribute to the chemical pollution, i.e., with initial masses below 20–25 $M_\odot$ (the more massive progenitors implode see Sect. 4.2.3 below). During this phase most of the first-generation stars that occupy the outer regions of the cluster are lost into the Galactic halo, while second-generation stars are more centrally concentrated and remain bound to the GC.
5. *Long-term dynamical evolution*. Later, the long-term relaxation-driven evaporation leads to the preferential loss of first-generation stars over 2–3 relaxation timescales (see Paper I). Finally, both populations are mostly mixed and no further evolution of the number ratio between first and second generation long-lived stars is possible (Paper I). Nowadays only the GC ω Cen keeps a memory of the different initial distributions between first and second generations stars, because the two-body relaxation time in the core is comparable to the cluster age.

[4] Note that in principle second generation massive stars could lead to the formation of a third generation of stars, but the higher order generations would only comprise an insignificant fraction of the whole population.

4.2. Possible issues

The scenario outlined above faces several issues that require further discussion.

4.2.1. Total star formation efficiency

The first issue is related to the dilution process between ISM and the ejecta of the polluters, and more specifically to the amount of pristine gas consumed to form second-generation stars. Indeed this process may change the total SFE, which is the main parameter affecting the efficiency of gas expulsion as discussed in Sect. 3.3.

Decressin et al. (2007a) determined that, in order to reproduce the Li-Na anticorrelation in NGC 6752, the mass ratio between pristine gas and slow stellar winds is around 1.15 after integration over time and IMF of the massive star polluters. On the other hand, the mass lost by massive stars and recycled into the second generation represents only 3.5–4% of the total mass of the first generation stars. Thus for a star formation efficiency for the first generation of $\epsilon_{1G} = 0.33$, and assuming that all the matter ejected in the slow winds of the polluters is converted into stars with a dilution factor of 1.2 with pristine gas[5], we find that at most 1.32% of the protocluster gas is used to form the second sellar generation. Thus the SFE is only slightly modified (by a few percent) by the second episode of star formation. In other words, the SFE is mainly determined by the formation of the first stellar generation.

4.2.2. Initial mass of proto-GC clouds

We can now try to estimate the initial mass of the proto-gas clouds from which GCs are born. From the global value of the SFE (around 0.33) within the cluster-forming volume, the proto-gas cloud is about three times more massive than the total mass of created stars of first and second generation. To explain the high number of anomalous stars observed in present-day globular clusters (around 85% in NGC 6752, Decressin et al. 2007a; 70% in NGC 2808, Prantzos & Charbonnel 2006) a large fraction of the stars born in the cluster should have been lost from the cluster during its evolution. Decressin et al. (2007a) estimate that around 95% of first generation stars need to be lost in NGC 6752. Thus the initial mass of NGC 6752 should be at least 10 times more massive than its present-day mass. Given the luminosity of NGC 6752 (Harris 1996) and a mass-to-light ratio of $M/L_v = 3$, we evaluate its actual mass to be $\sim 3 \times 10^5\ M_\odot$. Thus the mass of the proto-gas cloud should have been of the order of $9 \times 10^6\ M_\odot$.

However, NGC 6752 is one of the most extreme cases of the anomalous stars. Carretta et al. (2009) statistically studied 19 GCs and find that stars with abundance anomalies (their intermediate and extreme populations) represent 50 to 80% of the cluster stars. Therefore NGC 6752 can be one of the most massive GCs initially, and the initial mass of most GCs is only several $10^6\ M_\odot$. These high stellar masses would explain why the pre-supernova feedback energy is not able to expel the gas from the cluster (Baumgardt et al. 2008).

4.2.3. Detailed chronology: early cluster evolution

One key issue concerns the necessity of retaining pristine gas within the cluster during the lifetime of the polluters in order to

[5] These assumptions are needed to maximise the initial number of second generation stars.

account for the presence of lithium in the atmosphere of second-generation stars. This constraint is relevant for the question of whether very massive stars that produce the first SN are unable to clear out the cluster from its gas.

This condition can also be fulfilled if at the end of their lives the polluter stars do not undergo supernova explosions but rather directly collapse into black holes, avoiding injection of SN kinetic energy into the ISM. Observational clues from black hole X-ray binaries (Portegies Zwart et al. 1997; Ergma & van den Heuvel 1998), as well as nucleosynthesis constraints (Maeder 1992; Kobulnicky & Skillman 1997), suggest that black holes form from stars with masses above ~25 $M_\odot$ (see also Heger et al. 2003). This rough limit is confirmed by 2D core-collapse SN simulations (Fryer 1999), which also predict that progenitor stars more massive than ~40 $M_\odot$ are unable to launch shocks and thus do not produce an SN explosion. In view of the sensitivity of core collapse simulations to the (uncertain) input physics, these numbers must be considered with caution. For example, lowering the mean neutrino energy by 20% lowers the fallback black hole limit to ~15 $M_\odot$ (Fryer 1999). In addition, rotation is expected to decrease the lower mass limit for black hole formation (e.g., Hirschi et al. 2004). Besides, Georgy et al. (2009) find that the lowest masses to allow black hole formation decrease from 40 to 30 $M_\odot$ when the metallicity decreases from solar to $Z = 0.004$.

Despite the theoretical uncertainties regarding the formation of black holes and the physics of SN explosions, what matters at this level of the discussion is that the lower mass limit for a star to collapse directly into a black hole is very close to that of the fast-rotating massive polluter stars. This provides a natural way of avoiding the deposition of SN kinetic energy into the ISM for the first 7–10 Myr of GC evolution, and thus to retain pristine gas within the cluster during the lifetime of the polluters.

4.2.4. Detailed chronology: onset of gas expulsion

On the other hand, if all massive stars with initial mass below 25 $M_\odot$ end up as SN, we still have to check that they are numerous enough to expel the remaining pristine gas from the cluster potential well. Figure 4 (top panel) compares the binding energy for clusters with initial half-mass radii of 0.5 and 3 pc assuming an SFE of 0.33 with the energy released by all SNe for stars between 25 and 8 $M_\odot$ as a function of the cluster initial mass (gas and stars). These quantities are computed following Baumgardt et al. (2008). In the middle panel, we show the number of SNe needed to unbind both the cluster and the total number of SNe produced from stars in the mass range 25–8 $M_\odot$.

Both the binding and SN energies increase with the cluster mass but with different rates: the binding energy scales as $M_{\rm Tot}^2$, while the SN energy scales linearly. For clusters with mass below $10^{7.5}$ $M_\odot$ (i.e., the mass of proto-GC gas clouds), SN from stars in the mass range 8–25 $M_\odot$ produce enough energy for gas expulsion to operate.

4.2.5. Fast gas expulsion

Another issue concerns the timescale for gas expulsion, which has to be faster than the crossing time according to our scenario. To determine the timescale of gas expulsion by massive stars in the range 8–25 $M_\odot$ we present in Fig. 5 the SN rates we expect from a stellar population following a canonical IMF (Kroupa 2001) normalised to a 10^6 $M_\odot$ star cluster. We also indicate the total number of SNe the cluster has over time (bottom panel). After 30 Myr around 5000 SNe have exploded and even within 1 Myr after the 25 $M_\odot$ stars explode about 1000 SNe are produced.

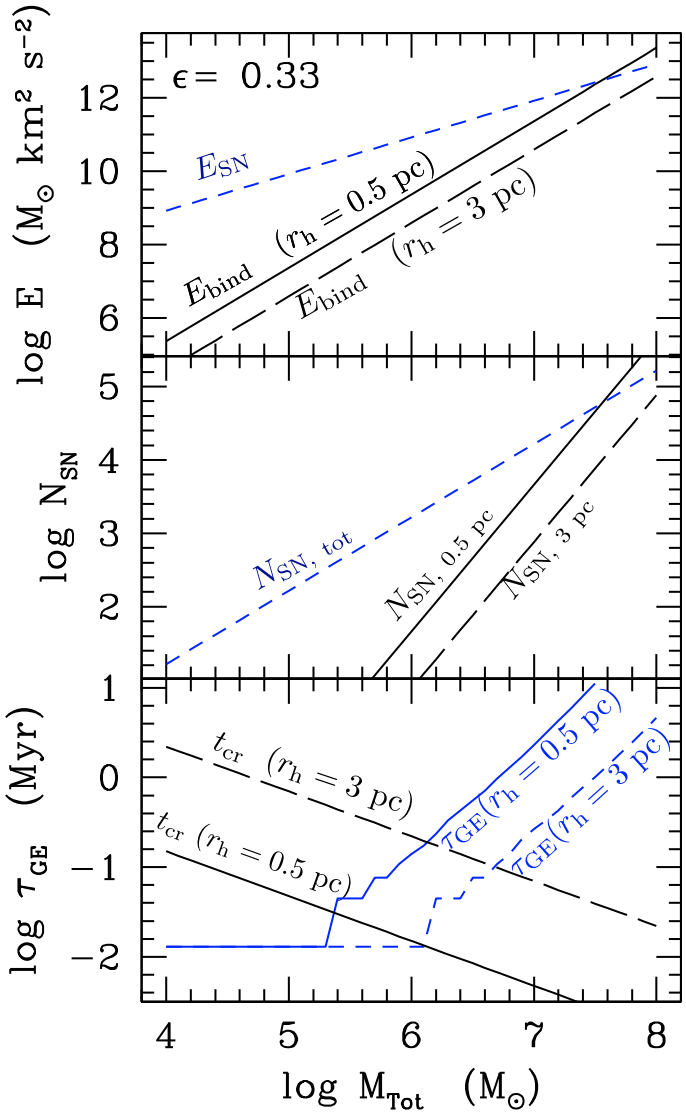

Fig. 4. *Top*: binding energy of a gas cloud as a function of its mass with an initial half-mass radius of 0.5 pc (full line) and 3 pc (long-dashed lines). The total energy released by SN for stellar progenitor masses between 8 and 25 $M_\odot$ is indicated as the short-dashed line. *Middle:* number of SNe needed to unbind a cluster as a function of its total mass with an initial half-mass radius of 0.5 pc (full line) and 3 pc and the total number of SNe created by the cluster (in the mass range 8–25 $M_\odot$). *Bottom*: crossing time of a cluster as a function of its total mass with an initial half-mass radius of 0.5 pc (full line) and 3 pc (long-dashed line) and corresponding gas expulsion timescale (full line and short-dashed line, e.g., Baumgardt et al. 2008).

We can now compare the time at which enough SNe are produced to unbind a cluster to the crossing time of the cluster. This result is shown in Fig. 4 (bottom panel) where both timescales are indicated. For clusters with small half-mass radii (around 0.5 pc), only clusters with initial mass below a few 10^5 $M_\odot$ experience fast gas expulsion as needed. However such a mass is too low to be the initial mass of GCs. On the other hand, clusters with large half-mass radii (around 3 pc) can produce fast gas expulsion up to a mass of 5×10^6 $M_\odot$, which is consistent with the value we infer for most proto-GCs. In the extreme case of NGC 6752 (with mass up to 9×10^6 $M_\odot$, see Sect. 4.2.2), the

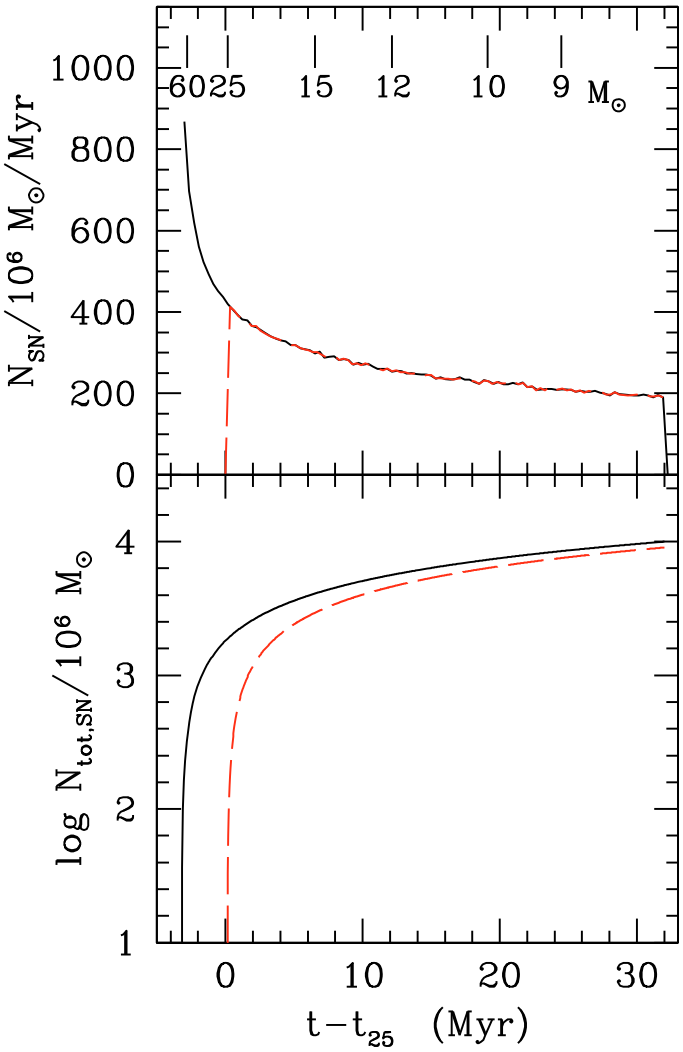

Fig. 5. *Top*: supernova rate as a function of time, using the Hurley et al. (2000) stellar-evolution routines, for a single stellar population of 10^6 $M_\odot$ following a canonical IMF. Full and dotted lines refer to cases where all stars above 8 $M_\odot$ produce an SN or only stars in the mass range 25–8 $M_\odot$, respectively. *Bottom*: integration over time of the number of SNe. In both panels time is shifted to the SNe produced by stars with an initial mass of 25 $M_\odot$.

initial half-mass radius should be about of 3–5 pc to allow a fast enough gas expulsion.

This confirms the results of Parmentier & Fritze (2009), who show that, for clusters with mass around 10^6–10^7 $M_\odot$, gas expulsion is more likely to happen in 2 or 3 crossing times, implying an adiabatic regime (i.e., small radius). Besides, our findings are mainly compatible with the ones of Marks et al. (2008, 2010), which explains the relation between the slope of the actual mass function and the concentration of GCs as the dynamical response for the gas expulsion process. However, the initial mass and radius of the cluster found by Marks et al. (2010) are smaller than the ones obtain in this paper as they deduced a top-heavy IMF to obtain gas expulsion.

4.2.6. Place of birth of second-generation stars

Let us now address the issue of how the slow winds of fast-rotating massive stars are recycled into second-generation stars. Decressin et al. (2007b) assume that the matter inside the equatorial disc can already start to condense and produce a proto-stellar object. However this local formation of second-generation stars cannot allow the formation of a distinct main sequence as observed in ω Cen (Bedin et al. 2004) and NGC 2808 (Piotto et al. 2007), as pointed out by Decressin et al. (2007a) and Renzini (2008).

However, it is possible that the strong radiation pressure accelerates the disc so that it dissipates on larger scales. Here we assumed that the disc is dense enough so that stellar radiation is not able to accelerate the matter above the escape velocity of the cluster. The matter originating in the disc will be stored outside the cluster centre and will fall back when it is cold enough. The main difficulty of this scenario is to prevent the mixing between SN ejecta with these slow winds. This can be the case if the ISM (and the diluted slow winds) present inhomogeneities such that SN ejecta escape the cluster mainly through low-density regions creating tunnels (see Prantzos & Charbonnel 2006). A similar view is presented by Palouš et al. (2009): thermal instabilities developed when the energy deposition to the ISM is dominated by stellar winds (with H-burning products). A large part of the matter sinks into the cluster centre in the form of compact high density and cold gas, which can be used to form second-generation stars. Later when SNe dominate the input energy, the cluster is cleared out by a stationary outflow (see also Tenorio-Tagle et al. 2007; Wünsch et al. 2008).

In this case it will be possible that the slow component (i.e. the slow winds enriched with H-burning matter) remains decoupled from the SN ejecta and cools down so that it migrates towards the cluster centre. There the pressure of the ISM increases and second-generation stars form. In this case second-generation stars will have a much more homogeneous chemical composition compared to the stochastic formation process near their massive progenitors. Therefore this scenario may reproduce the discrete He-sequences inferred from observations. However, the continuous O-Na distribution found in many clusters still offer a challenge (see e.g., Carretta et al. 2009).

5. Conclusions

In this paper we have studied the influence of primordial gas expulsion by supernovae during the early dynamical evolution of GCs in the context of clusters with two chemically and dynamically distinct stellar populations. In particular, we investigated whether this dynamical process can explain the high number of observed second generation stars that harbour abundance anomalies in light elements. We deduced the following.

- If the two populations have a different radial extent with second-generation stars more concentrated, primordial gas expulsion is able to expel most of the first-generation stars, while most second-generation stars can be retained.
- For a given fractional mass loss by the cluster, the fraction of second-generation stars is nearly independent of the gas expulsion parameters (see Sect. 3.2).
- The final observed fraction of second-generation stars can constrain the initial properties of GCs, as this fraction is highest for clusters with SFE around 0.3–0.33, with concentrated clusters relative to the tidal field, and with a fast timescale for gas expulsion relative to the crossing time.
- We infer proto-GC cloud masses of several 10^6 $M_\odot$ and up to 9×10^6 $M_\odot$ for clusters that show a large fraction of chemically different second generation stars like NGC 6752. Their initial half-mass radii are in the range of ~1–3 pc (4–5 pc for the most massive cases).

– It is possible to reproduce the fraction of second-generation stars in present-day GCs through cluster dynamical processes by combining gas expulsion and tidal stripping during long-term evolution of initially mass-segregated clusters.
– The primordial gas expulsion process can also be at the origin of the observational trend observed by Carretta (2006), who shows that clusters with a long orbital period and with high orbital inclinations relative to the Galactic plane produce more extended O-Na and Mg-Al anticorrelations.

Acknowledgements. T.D. and C.C. acknowledge financial support from the French Programme National de Physique Stellaire (PNPS) of the CNRS/INSU, and from the Swiss National Science Foundation (FNS).

References

Aarseth, S. J. 1999, PASP, 111, 1333
Arnould, M., Goriely, S., & Jorissen, A. 1999, A&A, 347, 572
Baumgardt, H., & Kroupa, P. 2007, MNRAS, 380, 1589
Baumgardt, H., Kroupa, P., & Parmentier, G. 2008, MNRAS, 384, 1231
Bedin, L. R., Piotto, G., Anderson, J., et al. 2004, ApJ, 605, L125
Bekki, K., Campbell, S. W., Lattanzio, J. C., & Norris, J. E. 2007, MNRAS, 267
Bellini, A., Piotto, G., Bedin, L. R., et al. 2009, A&A, 507, 1393
Bonifacio, P., Pasquini, L., Molaro, P., et al. 2007, A&A, 470, 153
Brown, J. A., & Wallerstein, G. 1993, AJ, 106, 133
Caloi, V., & D'Antona, F. 2005, A&A, 435, 987
Caloi, V., & D'Antona, F. 2007, A&A, 463, 949
Carretta, E. 2006, AJ, 131, 1766
Carretta, E., Bragaglia, A., Gratton, R. G., et al. 2006, A&A, 450, 523
Carretta, E., Bragaglia, A., Gratton, R. G., Lucatello, S., & Momany, Y. 2007, A&A, 464, 927
Carretta, E., Bragaglia, A., Gratton, R., & Lucatello, S. 2009, A&A, 505, 139
Cottrell, P. L., & Da Costa, G. S. 1981, ApJ, 245, L79
de Mink, S. E., Pols, O. R., Langer, N., & Izzard, R. G. 2009, A&A, 507, L1
Decressin, T., Charbonnel, C., & Meynet, G. 2007a, A&A, 475, 859
Decressin, T., Meynet, G., Charbonnel, C., Prantzos, N., & Ekström, S. 2007b, A&A, 464, 1029
Decressin, T., Baumgardt, H., & Kroupa, P. 2008, A&A, 492, 101
Decressin, T., Charbonnel, C., Siess, L., et al. 2009, A&A, 505, 727
Denissenkov, P. A., & Herwig, F. 2003, ApJ, 590, L99
D'Ercole, A., Vesperini, E., D'Antona, F., McMillan, S. L. W., & Recchi, S. 2008, MNRAS, 1228
Ergma, E., & van den Heuvel, E. P. J. 1998, A&A, 331, L29
Fenner, Y., Campbell, S., Karakas, A. I., Lattanzio, J. C., & Gibson, B. K. 2004, MNRAS, 353, 789
Fraix-Burnet, D., Davoust, E., & Charbonnel, C. 2009, MNRAS, 398, 1706
Fryer, C. L. 1999, ApJ, 522, 413
Georgy, C., Meynet, G., Walder, R., Folini, D., & Maeder, A. 2009, A&A, 502, 611
Gratton, R., Sneden, C., & Carretta, E. 2004, ARA&A, 42, 385
Gratton, R. G., Lucatello, S., Bragaglia, A., et al. 2007, A&A, 464, 953
Harris, W. E. 1996, AJ, 112, 1487
Heger, A., Fryer, C. L., Woosley, S. E., Langer, N., & Hartmann, D. H. 2003, ApJ, 591, 288
Herwig, F. 2004a, ApJ, 605, 425
Herwig, F. 2004b, ApJS, 155, 651
Hirschi, R., Meynet, G., & Maeder, A. 2004, A&A, 425, 649
Hurley, J. R., Pols, O. R., & Tout, C. A. 2000, MNRAS, 315, 543
Karakas, A. I., & Lattanzio, J. C. 2003, Publications of the Astronomical Society of Australia, 20, 279
Kobulnicky, H. A., & Skillman, E. D. 1997, ApJ, 489, 636
Kraft, R. P. 1994, PASP, 106, 553
Kroupa, P. 2001, MNRAS, 322, 231
Lada, C. J., & Lada, E. A. 2003, ARA&A, 41, 57
Lind, K., Primas, F., Charbonnel, C., Grundahl, F., & Asplund, M. 2009, A&A, 503, 545
Maeder, A. 1992, A&A, 264, 105
Marks, M., Kroupa, P., & Baumgardt, H. 2008, MNRAS, 386, 2047
Marks, M., Kroupa, P., & Baumgardt, H. 2010, MNRAS, in press
Milone, A. P., Piotto, G., King, I. R., et al. 2010, ApJ, 709, 1183
Palouš, J., Wünsch, R., Tenorio-Tagle, G., & Silich, S. 2009, in IAU Symp. 254, ed. J. Andersen, J. Bland-Hawthorn, & B. Nordström, 233
Paresce, F., & De Marchi, G. 2000, ApJ, 534, 870
Parmentier, G., & Fritze, U. 2009, ApJ, 690, 1112
Pasquini, L., Bonifacio, P., Molaro, P., et al. 2005, A&A, 441, 549
Pasquini, L., Bonifacio, P., Randich, S., et al. 2007, A&A, 464, 601
Pflamm-Altenburg, J., & Kroupa, P. 2009, MNRAS, 397, 488
Piotto, G., Villanova, S., Bedin, L. R., et al. 2005, ApJ, 621, 777
Piotto, G., Bedin, L. R., Anderson, J., et al. 2007, ApJ, 661, L53
Portegies Zwart, S. F., Verbunt, F., & Ergma, E. 1997, A&A, 321, 207
Prantzos, N., & Charbonnel, C. 2006, A&A, 458, 135
Prantzos, N., Charbonnel, C., & Iliadis, C. 2007, A&A, 470, 179
Renzini, A. 2008, MNRAS, 391, 354
Smith, G. H. 2006, PASP, 118, 1225
Tenorio-Tagle, G., Wünsch, R., Silich, S., & Palouš, J. 2007, ApJ, 658, 1196
Townsend, R. H. D., Owocki, S. P., & Howarth, I. D. 2004, MNRAS, 350, 189
Tutukov, A. V. 1978, A&A, 70, 57
Ventura, P., & D'Antona, F. 2005a, A&A, 431, 279
Ventura, P., & D'Antona, F. 2005b, A&A, 431, 279
Ventura, P., & D'Antona, F. 2005c, A&A, 439, 1075
Ventura, P., & D'Antona, F. 2008a, A&A, 479, 805
Ventura, P., & D'Antona, F. 2008b, MNRAS, 385, 2034
Ventura, P., & D'Antona, F. 2009, A&A, 499, 835
Ventura, P., D'Antona, F., Mazzitelli, I., & Gratton, R. 2001, ApJ, 550, L65
Ventura, P., D'Antona, F., & Mazzitelli, I. 2002, A&A, 393, 215
Villanova, S., Piotto, G., King, I. R., et al. 2007, ApJ, 663, 296
Wallerstein, G., Leep, E. M., & Oke, J. B. 1987, AJ, 93, 1137
Wünsch, R., Tenorio-Tagle, G., Palouš, J., & Silich, S. 2008, ApJ, 683, 683